

POWER FACTOR CORRECTION IN PERMANENT MAGNET BRUSHLESS DC MOTOR DRIVE USING SINGLE-PHASE CUK CONVERTER

SANJEEV SINGH*, BHIM SINGH

Electrical Engineering Department, Indian Institute of Technology Delhi,
Hauz Khas, New Delhi-110016, India

*Corresponding Author: sschauhan.sdl@gmail.com

Abstract

Permanent magnet brushless DC motor (PMBLDCM) drives are being employed in many variable speed applications due to their high efficiency, silent operation, compact size, high reliability, ease of control, and low maintenance requirements. These drives have power quality problems and poor power factor at input AC mains as they are mostly fed through diode bridge rectifier based voltage source inverters. To overcome such problems a single-phase single-switch power factor correction AC-DC converter topology based on a Cuk converter is proposed to feed voltage source inverters based PMBLDCM. It focuses on the analysis, design and performance evaluation of the proposed PFC converter topology for a 1.5 kW, 1500 rpm, 400 V PMBLDCM drive used for an air-conditioning system. The proposed PFC converter topology is modelled and its performance is simulated in Matlab-Simulink environment and results show an improved power quality and good power factor in wide speed range of the drive.

Keywords: PMBLDCM drive, Power factor correction, Cuk converter,
Air-conditioning, VSI.

1. Introduction

A permanent magnet brushless DC motor (PMBLDCM) is a kind of three-phase synchronous motor having permanent magnets on the rotor [1-5]. It is regarded as a rugged and efficient machine for variety of applications. Usually, the PMBLDCMs are powered from single-phase AC mains through a diode bridge rectifier (DBR) with smoothing DC capacitor and a three-phase voltage source inverter (VSI) [2-3, 5]. Due to the uncontrolled charging of DC link capacitor, the AC mains current waveform is a pulsed waveform featuring a peak value higher

Nomenclatures

C_o	Capacitor of the output ripple filter, μF
C_1	Intermediate capacitor, μF
D	Duty ratio
e_x	Back emf of phase x of PMBLDCM
f_s	Switching frequency, Hz
I_{av}	Average motor current from DC link, A
I_{dc}^*	Reference inductor current, A
I_s	Input AC Current (RMS), A
i_x	Current in phase x of PMBLDCM, A
J	Inertia of PMBLDC motor, kgm^2
K_b	Back EMF constant of the PMBLDCM
K_{pv}, K_{iv}	Proportional and integral gains of the voltage PI controller
K_{pw}, K_{iw}	Proportional and integral gains of the speed PI controller
k_{dc}	Gain
L_i	Boost inductor, mH
L_o	Inductance of output ripple filter, mH
L_s	Self-inductance of the PMBLDCM/phase
M	Mutual inductance of the PMBLDCM
m_d	Carrier waveform
P	Number of poles in the PMBLDCM
p	Differential operator (d/dt)
R	Equivalent Output Resistance at DC Link, Ω
R_a	Resistance of motor winding/phase, Ω
S	Switching function
T_e	Electromagnetic torque of PMBLDCM
T_l	Load torque on the PMBLDC motor
u_{vi}	Unit template of the input AC
V_{dc}^*	Reference DC link voltage, V
V_{dc}	Output voltage, V
V_{dc}	Sensed DC link voltage, V
V_e	Voltage error at DC Link, V
V_{in}	Output voltage of DBR, V
V_s	Input AC Voltage (RMS), V

Greek Symbols

ΔI_{Li}	Peak to peak current ripple in boost inductor, A
ΔI_{Lo}	Inductor peak to peak current ripple, A
ΔV_{Co}	Peak to peak ripple in output voltage, V
ΔV_{C1}	Peak to peak voltage ripple of intermediate capacitor, V
θ	Rotor position
ω	Frequency at input AC mains, rad/s
ω_r^*	Reference speed of the PMBLDCM, rad/s
ω_e	Speed error, rad/s
ω_r	Rotor speed of the PMBLDCM, rad/s

Abbreviations	
CCM	Continuous conduction mode
CF	Crest factor
DBR	Diode bridge rectifier
IGBTs	Insulated gate bipolar transistors
PF	Power factor
PFC	Power factor correction
PI	Proportional-integral
PMBLDCM	Permanent magnet brushless DC motor
PQ	Power quality
PWM	Pulse width modulation
THD	Total harmonic distortion
VSI	Voltage source inverters

than the peak of the fundamental input current as shown in Fig. 1. The power factor (PF) is 0.738, crest factor (CF) is 2.24 with 67% efficiency of the drive.

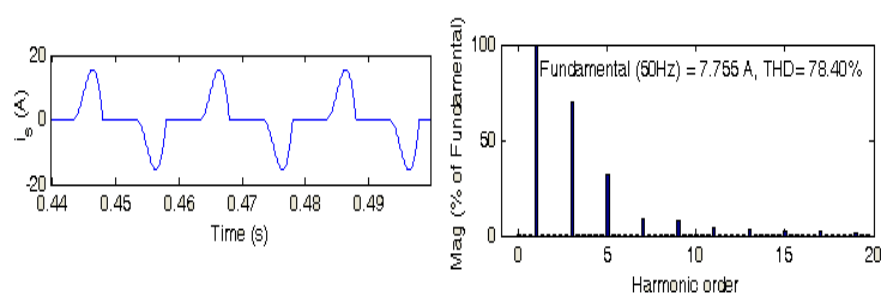


Fig. 1. Supply Current and Harmonic Spectrum (at 220 V_{AC}) of a DBR Fed PMBLDCM Drive at Rated Torque and 1000 rpm.

This is due to the fact that, the DBR does not draw any current from the AC mains when the AC voltage is less than the DC link voltage, as the diodes are reverse biased during that period; however, it draws a large current when the AC voltage is higher than the DC link voltage. Therefore, many power quality (PQ) problems arise at input AC mains including poor power factor, increased total harmonic distortion (THD) and high crest factor (CF) of AC mains current etc. These PQ problems become more severe for the utility when many such drives are employed simultaneously at various places.

To mitigate PQ and associated problems several international standards have come up in the recent past including IEC 61000-3-2 [6] which is specially meant for low power drives. Therefore, the drive system having inherent power factor correction (PFC) are more in demand and PFC converters have become preferred feature of new drives. Since the PMBLDCM drives have to be operated from the utility supply, therefore they should conform to the international PQ standards.

To comply with the PQ standards in the low power range, the power factor correction (PFC) converter topology using active wave shaping techniques is a popular and preferred solution in domestic applications. The PFC converter forces the drive to draw sinusoidal AC mains current in phase with its voltage.

Moreover, for PFC converter fed PMBLDCM drives, the additional cost and complexity of the PFC converter are not justified, therefore, converter topologies with inherent feature of PFC are preferred in these drives. Therefore, a DC-DC converter topology is mostly preferred amongst several available topologies [7-15] e.g., buck, boost, buck-boost, Cuk, SEPIC, zeta converters with variations of capacitive/inductive energy transfer. The net result is improved performance, such as reduction of AC mains current harmonics, reduction of acoustic noise and electromagnetic pollution, minimum number of components, enhanced efficiency, utilization of the full input voltage range etc.

Few efforts [9,11,13,15] have been made to introduce PFC feature in PMBLDC motors using unipolar excitation [13] and bipolar excitation [9,11,15] of PMBLDCMs. For air-conditioners, a PMBLDCM with boost PFC converter [11] and PMSM with improved power quality converter [12] have been reported for power quality improvement. However, a PMBLDCM is best suited for air-conditioning system due to simple control, high average torque produced and few torque ripples.

This paper deals with a Cuk converter as PFC AC-DC converter to feed PMBLDCM driven air-conditioner. Because, the Cuk converter with PFC inherits advantages like low current and voltage ripple in output, near unity power factor with simple control and reduced size magnetics [7]. A detailed design and performance evaluation of the proposed PFC converter for feeding PMBLDCM drive are presented for air-conditioning system. The paper is organized in six main parts, namely introduction, operation and control of Cuk converter fed PMBLDCM, their design, modeling of the proposed PMBLDCM drive, performance evaluation and conclusion.

2. Operation and Control of Cuk Converter fed PMBLDCM

Figure 2 shows the proposed topology of Cuk PFC converter fed PMBLDCM drive with control scheme for the speed control as well as PFC with DC link voltage control. For the speed control of the PMBLDCM, a proportional-integral (PI) controller [3] is used to drive a constant torque compressor in air-conditioning system. The rotor position of PMBLDCM is sensed using Hall effect sensors and converted to speed signal, which is compared with a reference speed.

The speed error signal is passed through a speed controller to give the torque equivalent which is converted to current equivalent signal. This signal is multiplied with a rectangular unit template in phase with top flat portion of motor's back EMF to get reference currents of the motor. The reference motor currents are compared with the sensed motor currents. These current errors are amplified and amplified signals are then compared with triangular carrier wave to generate the PWM pulses for turning on/off the VSI switches. The control of PMBLDCM requires rotor-position information only at the commutation points, e.g., every 60° electrical in the three-phases [1-5], therefore, comparatively simple controller is required for commutation and current control.

The Cuk PFC converter topology has a conventional DBR fed from single-phase AC mains followed by the Cuk DC-DC converter, an output ripple filter and a three-phase VSI to feed the PMBLDC motor. The DC-DC converter provides a controlled DC voltage from uncontrolled DC output of DBR, while controlling the power factor (PF) through high frequency switching of the PFC

switch. The regulated output DC voltage from the DC-DC converter is decided by its duty ratio (D). The switching frequency (f_s) is decided by the switching device used, operating voltage, power level and switching losses of the device. In this work, a set of insulated gate bipolar transistors (IGBTs) are used as the switching devices in the PFC switch as well as in VSI bridge, because IGBTs can operate in wide switching frequency range to make optimum balance between magnetics, size of filter components and switching losses.

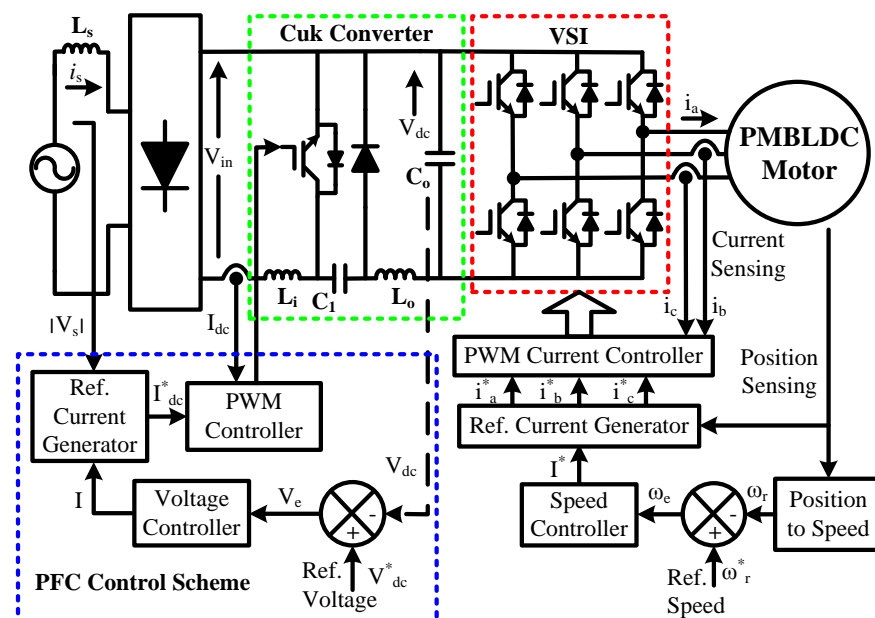


Fig. 2. Control Schematic of PFC Cuk Converter Fed PMBLDCM Drive.

The use of current multiplier approach with average current control scheme in continuous conduction mode (CCM) of the PFC converter makes this topology an efficient option. The control loop employed to execute PFC action involves outer voltage loop and inner current loop. For control action, the DC link voltage is sensed and compared with the set reference voltage at DC link. The error voltage is passed through a voltage PI controller to give the modulating current signal. This signal is multiplied with a unit template of input AC voltage which is compared with DC current sensed after the DBR. Hall effect voltage and current sensors are employed for voltage and current sensing. This current error is amplified and amplified signal is then compared with sawtooth carrier wave to generate the PWM pulses for turning on/off the DC-DC converter switch. The complete control strategy consists of selection of sensors, design of control algorithm and PWM controller for the drive.

3. Design of Cuk PFC Converter for PMBLDCM

Figure 2 shows the proposed topology of Cuk converter fed PMBLDCM drive. In the Cuk converter, the inductance, L_o , of output ripple filter restricts the inductor peak to peak current ripple, ΔI_{L_o} , within specified value for a given switching frequency, f_s . The capacitor, C_o , of the output ripple filter is considered to be very

large for ripple free output voltage. However, in practical situations the output voltage cannot be ripple free due to finite value of the capacitor, C_o , which can be calculated for a specified ripple in output voltage, ΔV_{Co} . Suitable snubbers are also designed for active switches along with the input and output ripple filters.

The Cuk converter belongs to the buck-boost converter family and has inverted voltage polarity at the output. It operates on the principle of capacitive energy transfer and uses inductors on both sides of the switch to reduce current ripple [7,10]. The Cuk DC-DC converter provides a regulated DC output voltage for wide range of input DC voltage. It is designed for constant voltage across the intermediate capacitor, C_1 , as it operates on the principle of capacitive energy transfer. The boost inductor, L_i , output filter inductor, L_o , and capacitor, C_o , are designed according to maximum allowable current and voltage ripple during transient conditions of the PMBLDCM drive. The design equations governing the duty ratio and other component values are as follows.

$$\text{Output voltage} \quad V_{dc} = \frac{DV_{in}}{1-D} \quad (1)$$

$$\text{Boost inductor} \quad L_i = \frac{DV_{in}}{f_s \Delta I_{Li}} \quad (2)$$

$$\text{Intermediate capacitor} \quad C_1 = \frac{D}{Rf_s \Delta V_{C1} / V_o} \quad (3)$$

$$\text{Output filter inductor} \quad L_o = \frac{(1-D)V_o}{f_s \Delta I_{Lo}} \quad (4)$$

$$\text{Output filter capacitor} \quad C_o = \frac{I_{av}}{2\omega \Delta V_o} \quad (5)$$

For $V_{dc} = 400$ V, $V_{in} = 198$ V for $V_{ac} = 220$ Vrms, $f_s = 40$ kHz, $I_{av} = 4$ A, $R = (V_o / I_{av}) = 100 \Omega$, $\Delta I_{Li} = 1.5$ A, $\Delta I_{Lo} = 2.0$ A (50% of I_{av}), $\Delta V_o = 4.25$ V (1.06% of V_o), $\Delta V_{C1} = 15$ V (3.75% of V_o), the design parameters are calculated on the basis of above equations as $L_i = 2.21$ mH, $C_1 = 4.45 \mu\text{F}$, $L_o = 1.6$ mH, $C_o = 1500 \mu\text{F}$.

4. Modeling of The Proposed PFC Converter for PMBLDCM Drive

The modeling of the proposed PFC converter fed PMBLDCM drive involves modeling of a PFC converter and modeling of PMBLDCM drive. The PFC converter consists of a DBR at front end and a Cuk converter with output ripple filter. Therefore, its modeling mainly includes the modeling of the voltage controller, reference current generator and PWM controller. The various components of PMBLDCM drive are a speed controller, a reference current generator, a PWM current controller and a PMBLDC motor. Each of the above components of a PMBLDCM drive are modeled by mathematical equations and combination of such models represent complete PMBLDCM drive.

4.1. PFC converter

The modeling of a PFC converter mainly consists of the modeling of the voltage controller, reference current generator and a PWM controller. These components require various signals sensed from the system e.g. DC link voltage, current after

DBR and input voltage template. The accuracy of the controller depends on these sensed signals.

4.1.1. Voltage controller

The modeling of a voltage controller is of prime importance as the performance of the PMBLDCM drive depends on this controller. The proportional integral (PI) controller is used to control the DC link voltage. At k^{th} instant of time, $V_{dc}^*(k)$ is reference DC link voltage, $V_{dc}(k)$ is sensed DC link voltage then the voltage error $V_e(k)$ is calculated as,

$$V_e(k) = V_{dc}^*(k) - V_{dc}(k) \quad (6)$$

This voltage error is processed through the voltage controller to get desired control signal. The output of the PI controller at k^{th} instant $I(k)$ is given as,

$$I(k) = I(k-1) + K_{pv}[V_e(k) - V_e(k-1)] + K_{iv}V_e(k) \quad (7)$$

where K_{pv} and K_{iv} are the proportional and integral gains of the voltage controller.

4.1.2. Reference current generator

The reference inductor current, I_{dc}^* , of the Cuk converter is given as,

$$I_{dc}^* = I(k)u_{vi} \quad (8)$$

where u_{vi} is the unit template of the input AC mains voltage calculated as,

$$u_{vi} = \frac{V_d}{V_{in}}; V_d = |V_i|; V_i = V_{in} \sin \omega t \quad (9)$$

where ω is frequency in rad/s at input AC mains.

4.1.3. PWM controller

The reference Cuk converter current is compared with its sensed current to generate the current error $\Delta i_{dc} = I_{dc}^* - I_{dc}$. This current error is amplified by gain k_{dc} and compared with carrier waveform $m_d(t)$. The switching signals for the IGBT of the PFC converter are generated by comparing this amplified current error with saw-tooth carrier waveform of 20 kHz.

$$\text{If } k_{dc} \Delta i_{dc} > m_d(t) \text{ then } S = 1 \quad (10)$$

$$\text{If } k_{dc} \Delta i_{dc} \leq m_d(t) \text{ then } S = 0 \quad (11)$$

where S is the switching function of the switch used in Cuk converter representing 'on' position with $S = 1$ and its 'off' position with $S = 0$.

4.2. PMBLDCM drive

The modeling of a speed controller is quite important as the performance of the system depends on this controller. If at k^{th} instant of time, $\omega_r^*(k)$ is reference speed, $\omega_r(k)$ is rotor speed then the speed error $\omega_e(k)$ can be calculated as,

$$\omega_e(k) = \omega_r^*(k) - \omega_r(k) \quad (12)$$

This speed error is processed through a speed controller to get desired control signal.

4.2.1. Speed controller

The PI controller is the simplest and most commonly used speed controller. The output of the PI controller at k^{th} instant $T(k)$ is given as,

$$T(k) = T(k-1) + K_{p\omega}[\omega_e(k) - \omega_e(k-1)] + K_{i\omega} \omega_e(k) \tag{13}$$

where $K_{p\omega}$ and $K_{i\omega}$ are the proportional and integral gains of the speed controller.

4.2.2. Reference winding currents

The amplitude of stator winding current is as,

$$I^* = \frac{T(k)}{2K_b} \tag{14}$$

where K_b is the back emf constant of the PMBLDCM.

The reference phase currents of the motor winding are denoted by i_a^*, i_b^*, i_c^* , for phases a, b, c respectively. For duration of 0-60° the reference currents can be given as,

$$i_a^* = I, i_b^* = -I, \text{ and } i_c^* = 0 \tag{15}$$

Similarly, the reference winding currents during other 60° duration are generated in rectangular 120° block form in phase with trapezoidal voltage of respective phases. These reference currents are compared with sensed phase currents to generate the current errors $\Delta i_a = (i_a^* - i_a), \Delta i_b = (i_b^* - i_b), \Delta i_c = (i_c^* - i_c)$ for three phases of the motor.

4.2.3. PWM current controller

The PWM current controller compares these amplified current errors of each phase with carrier waveform of a fixed frequency and generates the switching sequence for the voltage source inverter. These current errors $\Delta i_a, \Delta i_b, \Delta i_c$ are amplified by gain k_1 before comparing with carrier waveform $m(t)$. The switching sequence is generated based on the logic given for phase “a” as,

$$\text{If } k_1 \Delta i_a > m(t) \text{ then } S_a = 1 \tag{16}$$

$$\text{If } k_1 \Delta i_a \leq m(t) \text{ then } S_a = 0 \tag{17}$$

The switching sequences S_b and S_c are generated using similar logic for other two phases of the motor. For the projectile configuration comprising conical forebody and boattail, the effect

4.2.4. PMBLDC motor

The PMBLDC motor can be modeled in the form of a set of differential equations given as,

$$p i_x = (v_x - i_x R_a - e_x)/(L_s + M) \tag{18}$$

$$p\omega_r = (P/2) (T_e - T_i) / J \quad (19)$$

$$p\theta = \omega_r \quad (20)$$

The back emfs may be expressed as a function of position (θ) as,

$$e_x = K_b f_x(\theta) \omega_r \quad (21)$$

where x can be phase a , b or c and accordingly $f_x(\theta)$ represents function of rotor position with a maximum value ± 1 , identical to trapezoidal induced emf given as,

$$f_a(\theta) = 1 \quad \text{for } 0 < \theta < 2\pi/3 \quad (22)$$

$$f_a(\theta) = (6/\pi)(\pi - \theta) - 1 \quad \text{for } 2\pi/3 < \theta < \pi \quad (23)$$

$$f_a(\theta) = -1 \quad \text{for } \pi < \theta < 5\pi/3 \quad (24)$$

$$f_a(\theta) = (6/\pi)(\theta - 2\pi) + 1 \quad \text{for } 5\pi/3 < \theta < 2\pi \quad (25)$$

The functions $f_b(\theta)$ and $f_c(\theta)$ are similar to $f_a(\theta)$ with a phase difference of 120° and 240° respectively. Therefore, the electromagnetic torque expressed as,

$$T_e = K_b [f_a(\theta) i_a + f_b(\theta) i_b + f_c(\theta) i_c] \quad (26)$$

Equations (18-26) represent the model of the PMBLDC motor.

5. Performance Evaluation

The performance of the proposed PMBLDCM drive is evaluated for a compressor load of an air-conditioner in Matlab-Simulink environment. The compressor behaves as a constant torque equal to rated torque load and runs at variable speed as per requirement of air conditioning system. The PMBLDCM of 1.5 kW, 400 V rating, with 1500 rpm and 10 Nm torque is used to drive such load. The detailed data of the PMBLDC motor are given in *Appendix A*. The performance of the drive is simulated for constant rated torque (10 Nm) at reference speed of 1000 rpm. The DC link voltage is kept constant at 400 V with the input AC voltage of 220 V_{rms}. The components of Cuk converter are selected on the basis of PQ constraints at AC mains and allowable ripple in DC-link voltage as discussed in Section 3. The controller parameters have been tuned to get the desired PQ parameters and the values of controller gains are given in *Appendix A*. The performance evaluation is made on the basis of various PQ parameters i.e. current total harmonic distortion (THDi) at input AC mains, distortion factor (DF), displacement power factor (DPF), power factor (PF), crest factor (CF), input AC current rms value (I_{srms}) and efficiency of the drive.

5.1. Performance during starting

Figure 3(a) shows that the starting of the drive is smooth with rated torque (10 Nm) and PFC is achieved during the starting of the drive. The motor is started from 220 V_{rms} AC input at rated torque with a reference speed of 1000 rpm. The

maximum allowable torque and the stator current are limited to double the rated value. The motor speed reaches the reference speed within 0.2 s. Thereafter, the stator current and motor torque resumes the rated value within 0.01 s.

5.2. Performance during speed change

The speed is increased and decreased at rated torque for detailed evaluation of the drive as shown in Figs. 3(b)-(d). The motor speed is increased to 1200 rpm, as shown in Fig. 3(b) and decreased to 750 rpm, as shown in Fig. 3(c) from 1000 rpm. The motor attains the reference speed within couple of cycles of AC mains frequency during these changes. Moreover, the motor speed is reduced to 300 rpm (20% of its rated value) from 750 rpm within 0.02 s. while achieving the PFC at input AC mains, as shown in Fig. 3(d).

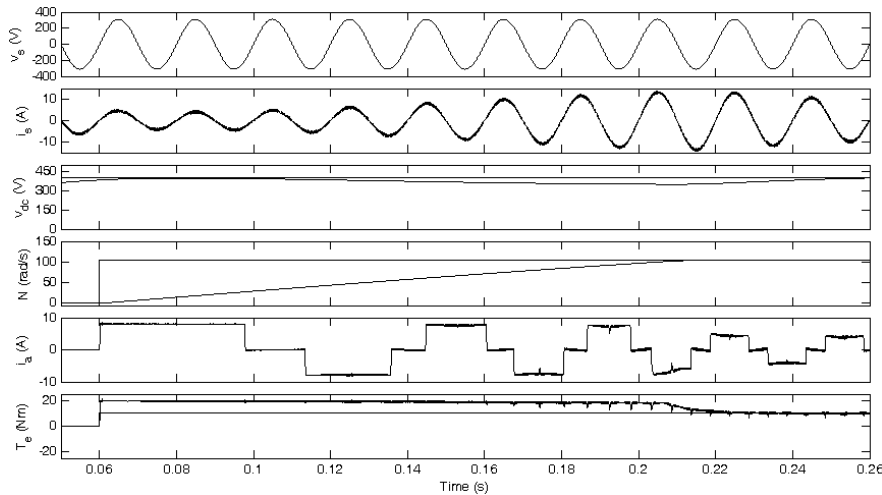


Fig. 3(a) Starting of PMBLDCM Drive at 1000 rpm (104.7 rad/s).

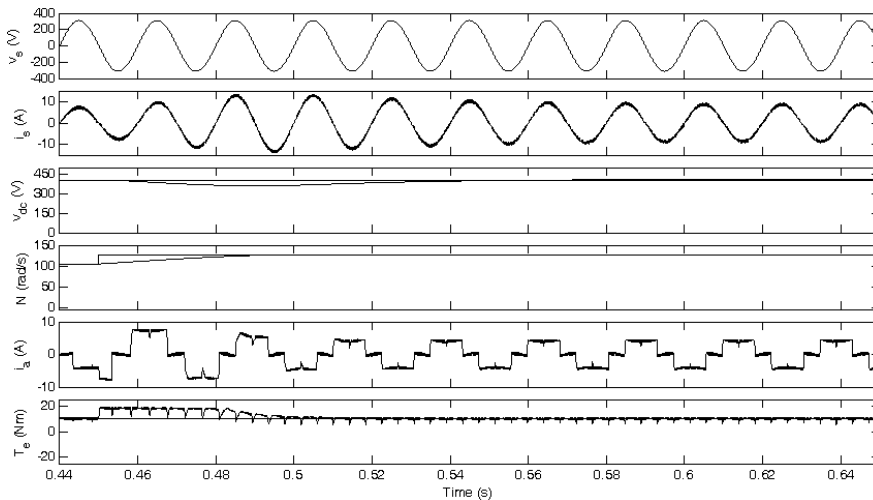


Fig. 3(b) Speed Change from 1000-1200 rpm (104.7- 125.7 rad/s).

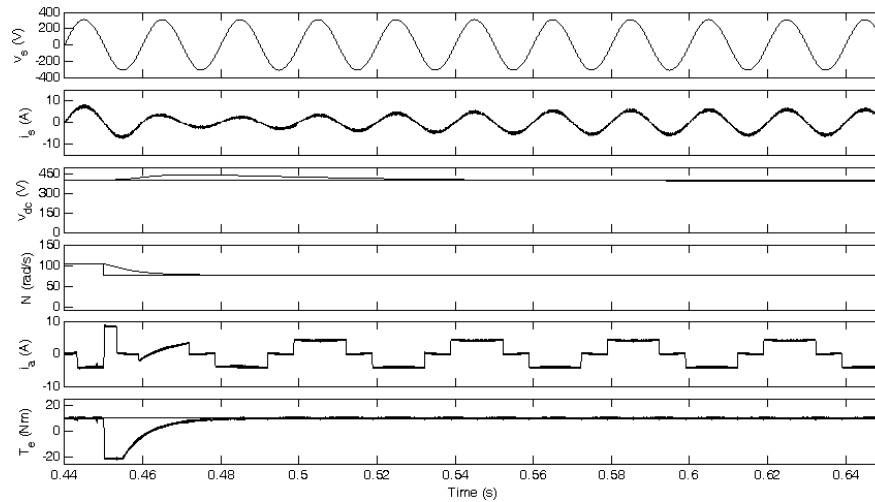


Fig. 3(c) Speed Change from 1000-750 rpm (104.7-78.5 rad/s).

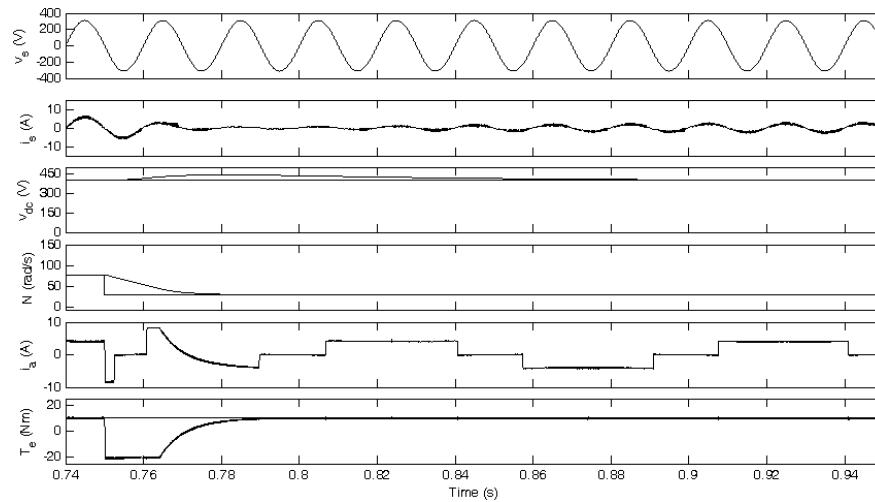


Fig. 3(d) Speed Change from 750-300 rpm (78.5-31.4 rad/s).

Fig. 3. Performance of a Cuk Converter Fed PMLDLCM Drive during Transient Conditions at Rated Torque (10Nm) with 220 VAC Input.

5.3. Performance during steady state condition

The current waveforms at AC input mains and its harmonic spectra during steady state at 1200 rpm, 1000 rpm, 750 rpm and 300 rpm are shown in Figs. 4(a)-(d). The current THD at AC mains remains less than 3% up to 50% of rated speed. However, the THD of AC mains current of the order of 5.57% is attained at 20% of rated speed with near unity power factor in the wide range of speed control. Moreover, the drive shows an improved performance in terms of reduced torque ripple, current ripple and speed ripple during steady state operating conditions.

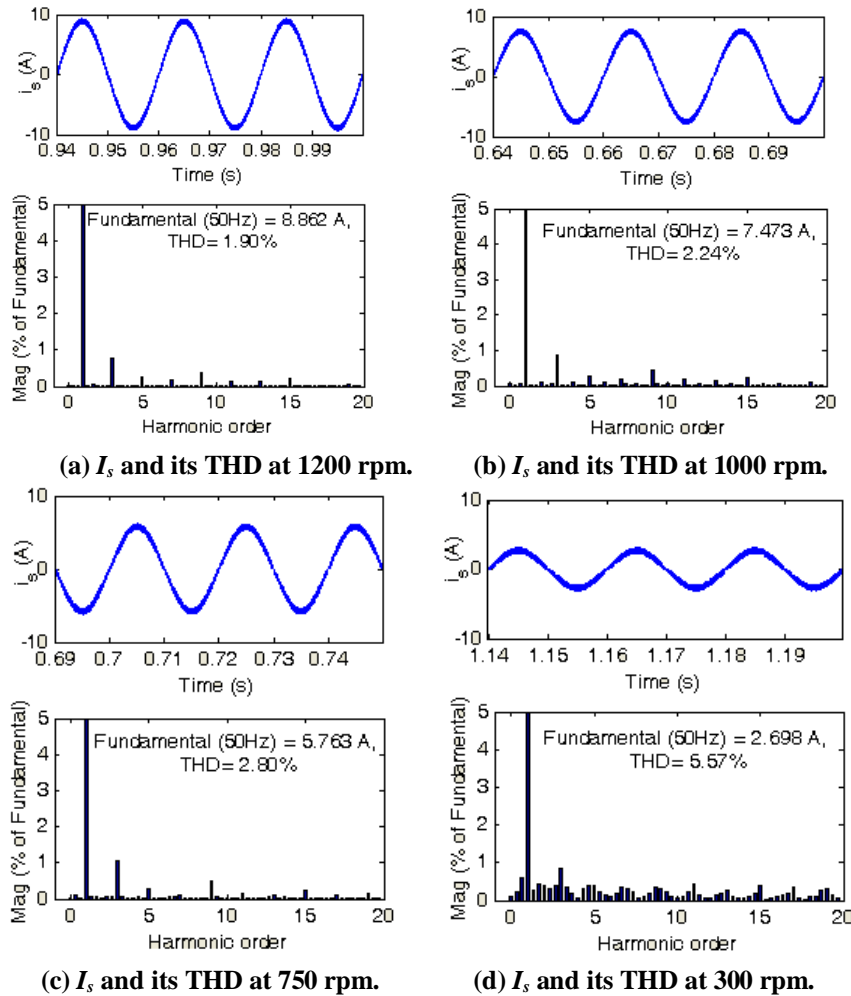


Fig. 4. Supply Current (I_s) Waveform and its Harmonic Spectra (at 220 V_{AC}) of a Cuk Converter Fed PMSBLDCM Drive During Steady-state Condition at Rated Torque.

5.4. Performance during input voltage variation

The variation of PQ parameters is observed for variable input AC voltages (170 V-270 V) with constant DC link voltage (400 V) to the drive for a speed of 1000 rpm as shown in Fig. 5. These results show reduced THD of AC mains current and improved PF in wide range of input AC voltage. The transient and steady state performances, current waveforms and its THD and PQ parameter variation with input voltage are shown in Figs. 3-5 to provide an exhaustive evaluation of the proposed topology. Moreover, the PQ parameters for variable AC input voltage are also shown in Table 1 for comparison. The current THD at input AC mains in steady state conditions always remains within the standards of IEC 61000-3-2 and the power factor remains near unity.

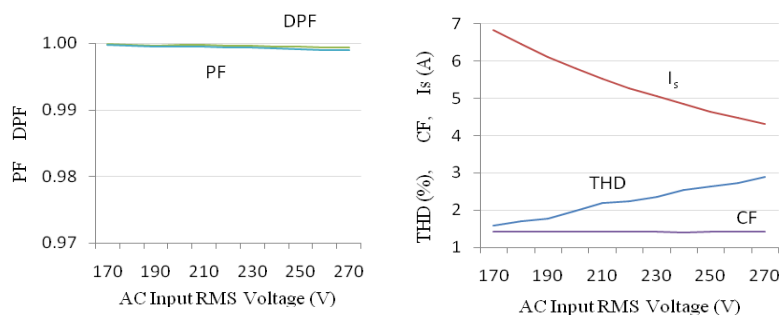


Fig. 5. Variation of PQ Parameters of a Cuk Converter Fed PMBLDCM Drive with Input Supply Voltage Variation (DC Link Voltage kept Constant at 400 V) at 1000 rpm Speed and Rated Torque (10 Nm).

Table 1. Variation of PQ Parameters with Input AC Voltage (V_{AC}) at 1000 rpm Speed and Rated Torque (10 Nm) with Constant DC Link Voltage (400 V).

V_{AC} (V)	THD _i (%)	DPF	PF	CF	I_s (A)	η_{Drive} (%)
170	1.59	0.9998	0.9997	1.41	6.83	91.2
180	1.69	0.9997	0.9996	1.41	6.45	91.1
190	1.78	0.9997	0.9995	1.41	6.11	91.1
200	1.97	0.9997	0.9995	1.41	5.81	91.1
210	2.19	0.9997	0.9995	1.41	5.53	91.1
220	2.24	0.9997	0.9994	1.42	5.28	91.1
230	2.36	0.9996	0.9993	1.41	5.05	91.0
240	2.53	0.9995	0.9992	1.41	4.85	91.0
250	2.63	0.9994	0.9991	1.41	4.65	91.0
260	2.73	0.9994	0.9990	1.41	4.48	90.9
270	2.90	0.9993	0.9989	1.41	4.31	90.8

6. Conclusion

A Cuk converter based PFC topology for a PMBLDCM drive has been proposed and validated for a compressor load of an air-conditioner. The PFC converter has ensured reasonable high power factor of the order of 0.998 in wide range of the speed as well as input AC voltage. Moreover, performance parameters show an improved power quality with less torque ripple, smooth speed control of the PMBLDCM drive. The THD of AC mains current has been observed well below 6% in most of the cases and completely satisfies the international norms [6]. The performance of the drive has been found very good in the wide range of input AC voltage with desired power quality parameters. This topology has been found suitable for the applications involving speed control at constant torque load.

References

1. Kenjo, T.; and Nagamori, S. (1985). *Permanent-magnet brushless DC motors*. Oxford University Press.
2. Sokira, T.J.; and Jaffe, W. (1989). *Brushless DC motors: Electronic Commutation and Control*. Tab Books USA.
3. Hendershort, J.R., Jr; and Miller, T.J.E. (1994). *Design of brushless permanent-magnet motors*. Oxford University Press, USA.

4. Gieras, J.F.; and Wing, M. (2002). *Permanent Magnet Motor Technology – Design and Application*. Marcel Dekker Inc., New York.
5. Pillay, P.; and Krishnan, R. (1989). Modeling, simulation and analysis of a permanent magnet brushless dc motor drives, part II: the brushless dc motor drive. *IEEE Trans. Ind. Appl.*, 25(2), 274-279.
6. International Standard IEC 61000-3-2, (2000). Limits for harmonic current emissions (Equipment input current ≤ 16 A per phase).
7. Brkovic, M.; and Cuk, S. (1992). Input current shaper using Cuk converter. *Proc. IEEE Telecommunications Energy Conference, 1992. INTELEC '92., 14th International*, 532 – 539.
8. Sebastian, J.; Cobos, J.A.; Lopera, J.M.; and Uceda, U. (1995). The determination of the boundaries between continuous and discontinuous conduction modes in PWM DC-to-DC converters used as power factor preregulators. *IEEE Trans. on Power Electronics*, 10(5), 574 – 582.
9. Tuckey, A.M.; and Patterson, D.J. (1996). The design and development of a high power factor current source controller for small appliance brushless DC motors. *Applied Power Electronics Conference and Exposition, 1996. APEC '96. Conference Proceedings 1996., Eleventh Annual*, 2, 778-781.
10. Simonetti, D.S.L.; Sebastian, J.; and Uceda, J. (1997). The discontinuous conduction mode Sepic and Cuk power factor preregulators: analysis and design. *IEEE Trans. Ind. Electron.*, 44(5), 630 – 637.
11. Singh, B.; Singh, B.P.; and Kumar, M. (2003). PFC converter fed PMBLDC motor drive for air conditioning. *Institution of Engineers (India) Journal-EL*, 84, 22-27.
12. Singh, B.; Murthy, S.S.; Singh, B.P.; and Kumar, M. (2003). Improved power quality converter fed permanent magnet AC motor for air conditioning. *Electric Power System Research*, 65(3), 239-245.
13. Gopalarathnam, T.; and Toliyat, H.A. (2003). A new topology for unipolar brushless dc motor drive with high power factor. *IEEE Trans. Power on Electronics*, 18(6), 1397-1404.
14. García, O.; Cobos, J.A.; Prieto, R.; Alou, P.; and Uceda, J. (2003). Single phase power factor correction: A survey. *IEEE Trans. Power on Electronics*, 18(3), 749-755.
15. Barkley, A.; Michaud, D.; Santi, E.; Monti, A.; and Patterson, D. (2006). Single stage brushless DC motor drive with high input power factor for single phase applications. *Power Electronics Specialists Conference, 2006. PESC '06. 37th IEEE*, 1-10.

Appendix A

PMBLDC Motor Data

Rated power	1.5 kW	Resistance R_s	2.8 Ω /ph.
Rated voltage	400 V _{DC}	Inductance (L_s+M)	5.21 mH/ph.
Rated speed	1500 rpm	Inertia J	0.013 kgm ²
Rated torque	10 Nm	Back EMF constant K_b	0.615 V s/rad
Poles	4		

The circuit parameters used for simulations: source impedance: 0.03 pu, switching frequency of PFC switch = 20 kHz. The gains of voltage and speed PI controllers: $K_{pv}= 0.09985$, $K_{iv}= 1.25$, $K_{p\omega}= 0.11$, $K_{i\omega}= 1.2$.